https://doi.org/10.31925/farmacia.2022.3.12 **ORIGINAL ARTICLE**

COMPATIBILITY STUDY BETWEEN MAGNESIUM OROTATE AND VARIOUS EXCIPIENTS IN THEIR PHYSICAL MIXTURES

CORINA MOISA [1], OANA CADAR [2], ERIKA ANDREA LEVEI [2], LAURA MUREȘAN [3], MARIANA GANEA [1], SEBASTIAN NEMETH [1], SIMONA CAVALU [4], LUCIANA DOBJANSCHI [4], MIHAELA ZDRINCA [4]*, REKA BARABAS [5], FLORIN BĂNICĂ [1]

[1]*University of Oradea, Medicine and Pharmacy Faculty, Department of Pharmacy, 29 Nicolae Jiga Street, 410028 Oradea, Romania*
[2]*INCDO-INOE 2000, Research Institute for Analytical Instrumentation, 67 Donath Street, 400293 Cluj-Napoca, Romania*
[3]*Babes-Bolyai University, "Raluca Ripan" Institute for Research in Chemistry, Fântânele Street 30, 400294 Cluj-Napoca, Romania*
[4]*University of Oradea, Medicine and Pharmacy Faculty, Department of Medical Disciplines, 1 Decembrie Street, 410028 Oradea, Romania*
[5]*Babeş-Bolyai University, Faculty of Chemistry and Chemical Engineering, 11 Arany Janos Street, 400028 Cluj-Napoca, Romania*

**corresponding author: mzdrinca@uoradea.ro*

Manuscript received: February 2022

Abstract

The assessment of magnesium orotate compatibility with various excipients is an important step in the development of drug formulation and development. A good physicochemical compatibility between magnesium orotate and different excipients allows obtaining novel combinations with a complex composition that enhances the therapeutic effect of magnesium orotate. The purpose of this research was to assess the compatibility of magnesium orotate with various excipients presently used in pharmaceutical formulations in a 1:1 mass ratio, which was higher than what was currently used in drug formulation, with the possibility of influencing the expected therapeutic benefit by delaying magnesium orotate release. The compatibility of the most used excipients (croscarmellose, corn starch, lactate, magnesium stearate, microcrystalline cellulose, polyvinyl-pyrrolidone and talcum) with magnesium orotate was assessed by investigating the TG–DTA-DTG curves, FTIR spectra and XRD pattern of the excipients and their physical mixture with magnesium orotate. A partial compatibility of magnesium orotate with corn starch, cellulose and croscarmellose was noticed based on thermal analysis. The FTIR spectra and TG-DTG results indicated the best stability of magnesium orotate in combination with polyvinyl-pyrrolidone, while a possible incompatibility between magnesium orotate and talcum was evidenced based upon FTIR spectra. No modifications in XRD pattern of magnesium orotate was noticed in the spectra corresponding to binary combinations. By corroborating the results, one can conclude that polyvinyl-pyrrolidone is the best choice as excipient for magnesium orotate.

Rezumat

Evaluarea compatibilității orotatului de magneziu cu diverși excipienți este un pas important în dezvoltarea formulării și dezvoltării medicamentelor. O bună compatibilitate fizico-chimică între orotatul de magneziu și diferiți excipienți permite obținerea unor combinații noi, cu o compoziție complexă, care sporește efectul terapeutic al orotatului de magneziu. Scopul acestui studiu a fost de a evalua compatibilitatea orotatului de magneziu cu diferiți excipienți utilizați în prezent în formulările farmaceutice, într-un raport masic 1:1, mai mare decât cel utilizat în prezent în formularea medicamentelor, cu o posibilă influență asupra efectului terapeutic așteptat, prin încetinirea eliberării orotatului de magneziu. Compatibilitatea celor mai utilizați excipienți (croscarmeloză, amidon de porumb, lactat, stearat de magneziu, celuloză microcristalină, polivinilpirolidonă și talc) cu orotatul de magneziu a fost evaluată prin investigarea curbelor TG-DTA-DTG, a spectrelor FTIR și a modelului XRD a excipienților și a amestecului lor fizic cu orotatul de magneziu. Pe baza analizei termice, s-a observat o compatibilitate parțială a orotatului de magneziu cu amidonul de porumb, celuloza și croscarmeloza. Spectrele FTIR și rezultatele TG-DTG au indicat cea mai bună stabilitate a orotatului de magneziu în combinație cu polivinilpirolidona, în timp ce o posibilă incompatibilitate între orotatul de magneziu și talc a fost evidențiată pe baza spectrelor FTIR. Nu s-a observat nici o modificare a modelului XRD al orotatului de magneziu în spectrele corespunzătoare combinațiilor binare. Prin coroborarea rezultatelor, se poate concluziona că polivinilpirolidona este cea mai bună alegere ca excipient pentru orotatul de magneziu.

Keywords: magnesium orotate, excipients, TG, DTA, DTG, XRD, FT-IR analysis

Introduction

In pharmaceutical practice, obtaining medicines with as much stability as possible over time, with high bio-availability, safety and innocuity is a priority that must be taken into account in the preparation of novel formulations. During processing and storage, medicines may undergo various physico-chemical or biological

interactions under the influence of internal and external factors [9]. As a result, there are various alterations in the quality of the active compounds, as well as a decrease of the pharmacological effects or even the appearance of toxic effects [23, 39].

A recent study indicated an increasing consumption of magnesium-based medicines both in children and in adults [17]. A large part of the population suffers from stress, sleep disorders and chronic fatigue, and magnesium deficiency occurs in 50% of these people. The recovery from magnesium deficiency depends on the source of magnesium used in therapy.

Magnesium is an essential cofactor for various metabolic reactions involving over 300 enzymes in the human body, being a cation with predominantly intracellular localization [4, 21, 25]. Magnesium dosing in the body is recommended in the assessment of renal function, diagnosis of gastrointestinal disorders, evaluation of electrolyte levels, investigation of neuromuscular activity, monitoring of heart diseases, monitoring of the response to the administration of magnesium supplements [7, 24]. Studies have shown good intracellular absorption of magnesium in the form of orotate compared to other magnesium compounds found in medicines used to restore optimal levels of magnesium in the body [18, 19].

The excipients used in our study are frequently employed in the pharmaceutical manufacture, being pharmaceutically pure and therefore we considered that there was no possibility of chemical reactions between components that would imply the existence of impurities. The therapeutical use of the selected excipients requires many studies related to the associated active substance, the existence or absence of the reactions between components. This study is an intermediate stage in the development of a new drug in which magnesium orotate will be associated with a soft matrix or fluid extract with possible hypolipidemic action that potentiates the therapeutic effect of magnesium orotate in stress condition and chronic fatigue. For this reason, we chose the 1:1 (w/w) ratio between magnesium orotate and the selected excipients, in a view of further investigations of magnesium orotate association with a soft matrix with possible lipid-lowering effect. Therefore, the lack of interaction between the excipient and the active substance is desired, while the excipient must have a good ability to retain the necessary moisture.

In order to obtain a higher bioavailability of the drug, it is important to avoid interactions between the components so that the active substance is released from the pharmaceutical form in a short time in order to obtain the desired therapeutic effect and to avoid possible gastric irritation due to an unsatisfactory disintegration of the pharmaceutical form in the digestive tract [27, 34, 37]. In this context, in order to assess the biocompatibility between magnesium orotate and different excipients currently used in pharmaceutical formulations and to identify possible chemical interactions between magnesium orotate and excipients, thermal analysis, FTIR spectroscopy and XRD pattern were employed, by characterizing the structural features of the physical mixture containing magnesium orotate and several excipients: croscarmellose, corn starch, lactate, magnesium stearate, microcrystalline cellulose, polyvinyl-pyrrolidone and talcum.

As there are largely available therapeutical formulations in which magnesium orotate is associated with different excipients, we chose to study the compatibility with these excipients in different mixtures with magnesium orotate, but in a higher mass ratio, in order to evaluate a possible negative effect on its release. A good compatibility between magnesium orotate and these excipients in a mass ratio of 1:1 may allow a further association of a soft or bioactive fluid extract with its own therapeutic action, in order to optimise existing formulations. Using an excess quantity of excipient compared to the current manufacture procedure, is intended to absorb any bioactive fluid extract in order to obtain an appropriate formulation.

Materials and Methods

Magnesium orotate was purchased from Merck (Darmstadt, Germany) and the excipients (corn starch, croscarmellose, lactate, magnesium stearate, microcrystalline cellulose, polyvinyl-pyrrolidone and talcum) were purchased from Sigma Aldrich (Taufkirchen, Germany).

Binary physical mixtures of magnesium orotate (MO) and each excipient were prepared under air atmosphere in a ratio of 1:1 (w/w), in a Retsch PM 200 Planetary Ball Mill for one hour, at 300 rpm, using agate jars and ball (10 nm). The resulted binary mixtures were as following: MO with croscarmellose (MO-CC), corn starch (MO-CS), lactate (MO-L), magnesium stearate (MO-S), microcrystalline cellulose (MO-C), polyvinyl-pyrrolidone (MO-PVP) and talcum (MO-T).

The XRD pattern of individual excipients and the binary mixtures were recorded using a Bruker D8 Advance diffractometer, operating at 40 kV and 40 mA, with CuKα radiation (λ = 1.5406 Å), at room temperature. The degree of crystallinity was calculated as the ratio between the area of all the diffraction peaks and the total area of the diffraction peaks and amorphous halo. Through XRD analysis it is possible to determine the interactions that occur during the pre-formulation process between MO and the excipients.

FT-IR spectroscopy was applied to identify possible interactions between MO and the studied excipients, using a Spectrum BX II spectrometer (PerkinElmer, Waltham, MA, USA) on KBr pellets containing 1% of each powder. FT-IR analysis can provide information on possible chemical interactions between MO and excipients. The absence of additional peaks indicates a proper compatibility of binary components in the mixture.

Thermal analysis was applied to identify the crystalline dehydration and melting transitions of the analytes being a rapid tool for investigating the compatibility between MO and excipients. A Mettler-Toledo TGA/ SDTA851 (Mettler-Toledo, Kowloon, Hong Kong) apparatus with a heating rate of 10°C/min under a nitrogen flow of 60 mL/min was used. All the thermal analysis experiments were performed in the temperature range of 25 - 500°C in alumina crucibles.

Results and Discussion

Thermal analysis

The thermal behaviour of MO and the TG-DTA-DTG curves are depicted in Figure 1. The decomposition of MO takes places in two well defined stages with a total mass loss of 59.2%. The first stage is observed in the temperature range 25 - 300ºC due to the elimination of two aqua ligands, with a mass loss of 9.98%, closed to the theoretical value (9.73%). This dehydration process is accompanied by an endothermic peak at 248°C. The results are in concordance with similar studies [31, 32]. The second stage corresponds to decomposition of MO with a loss of 49.2% observable in the temperature range 300 - 500°C. The endothermic shoulder at 372°C suggests that the MO decomposition occurs in successive steps.

The shoulder observed in the DTG/DTA curves is associated with the CO_2 release from the dissociation of orotate and formation of intermediary organic compounds, process which is accompanied by a mass loss of 12.55% (theoretical loss being 13.17%). Similar results were obtained by Yesilel *et al.* for the thermal analysis of the complex combination of orotic acid with Cu^{2+}, Ni^{2+}, Zn^{2+} and Cd^{2+} ions [26]. The literature survey did not provide any results related to the thermal decomposition of MO [42].

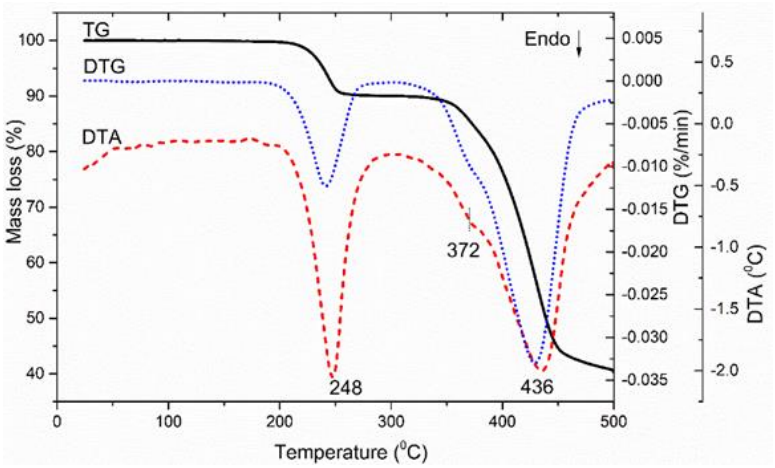

Figure 1.
TG, DTA and DTG curves of magnesium orotate

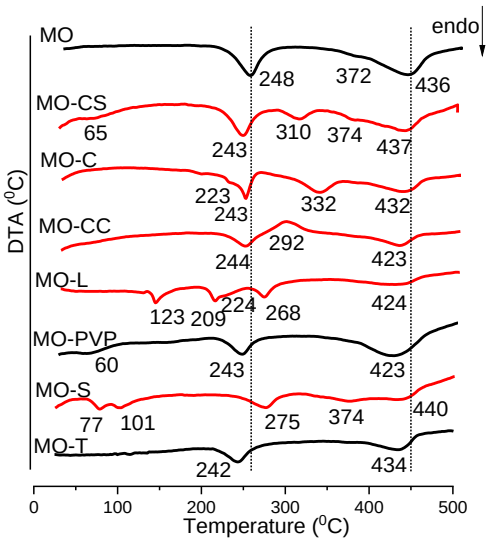

Figure 2.
DTA curves of MO and MO mixtures containing different excipients

The thermal behaviour of various mixtures of 1:1 mass ratio, containing MO and different excipients such as: corn starch (MO-CS), cellulose (MO-C), sodium croscarmellose (MO-CC), lactate (MO-L), povidone K 30 (MO-PVP), magnesium stearate (MO-S) and talc (MO-T) was analysed. Figure 2 shows the DTA curves of the above mentioned orotate mixtures.

Along with the two endothermic peaks visible at around 248°C and 436°C and attributed to MO, the DTA curves of the mixtures present several other peaks induced by the presence of the excipients. The observed features regarding the thermal effects of MO are confirmed by other studies in literature. For example, based on DSC investigations, Hassani A. *et al.* showed the presence of two endothermic peaks at ~240°C and ~ 477°C in MO [8].

The main thermal features of MO and MO mixtures are systematized in Table I along with the corresponding mass losses and DTG temperatures.

Table I

Thermal analysis results of MO and mixture of MO with different excipients

Sample	TG			DTG	DTA
	Mass Loss (%)	Temperature range (°C)	Mass loss (%)	T_{max} (°C)	T_{max}(°C)/thermal effect
MO	59.20	25 - 300	9.98	242	248
		300 - 500	49.22	372, 436	372/endo, 436/endo
MO-CS	71.28	25 - 150	4.29	54	65
		150 - 270	5.79	238	243
		270 - 350	32.37	308	310
		350 - 500	28.83	377, 429	374, 437
MO-C	75.75	25 - 270	7.33	236	223, 243
		270 - 370	43.10	329	332
		370 - 500	25.32	426	432
MO-CC	60.81	25 - 150	4.64	-	-
		150 - 260	6.42	239	244
		260 - 330	19.90	290	292
		330 - 500	29.85	422	423
MO-L	70.32	25 - 180	2.83	135	123
		180 - 250	9.60	228	209, 224
		250 - 350	27.62	269, 293	268
		350 - 500	30.27	421	424
MO-PVP	74.21	25 - 150	4.75	57	60
		150 - 300	6.58	242	243
		300 - 500	62.88	426	423
MO-S	73.84	25 - 150	2.73	74, 102	77, 101
		150 - 300	5.73	269	275
		300 - 420	48.56	371	374
		420 - 500	16.82	431	440
MO-T	29.87	25 - 300	4.98	242	224
		300 - 500	24.89	426	434

The effect of talcum and PVP on the thermal behaviour of MO is represented in Figure 3 based on the TG and DTG curves. Neither PVP or T does not affect the thermal behaviour of MO, however the mass loss of binary mixtures is lower (29.86%) in case of MO-T, compared to MO-PVP (74.21%).

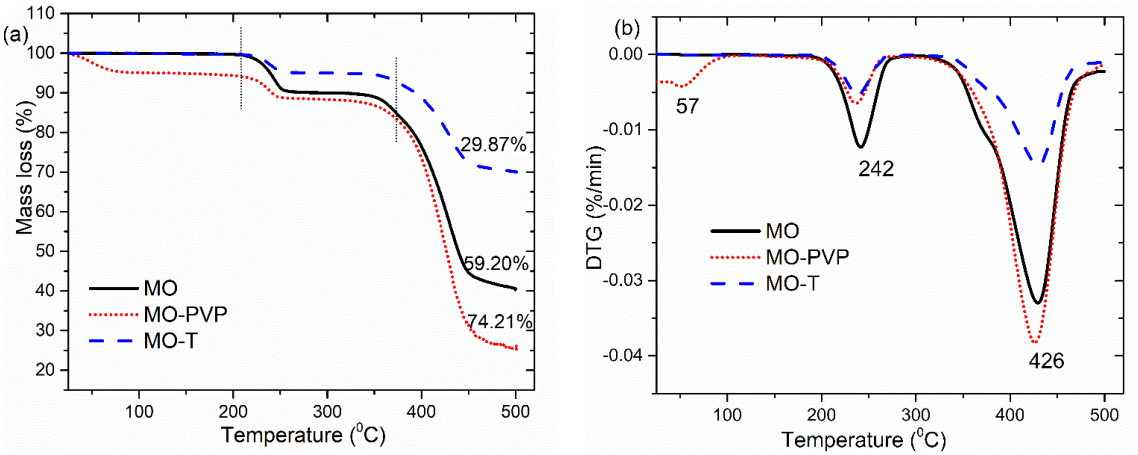

Figure 3.

TG (a) and DTG (b) curves of MO, MO-PVP and MO-T

In Figure 4 are depicted the TG and DTG curves of binary mixtures of MO with CS, C and CC. The total mass loss is between 71% and 81% with similar decomposition steps for all three excipients. It can be noticed the appearance of a new stage in the range 250 - 350°C, emphasized in Figures 4a, 4b and 4c, and attributed to the decomposition of excipients at 308°C (CS); 329°C (C) and 290°C (CC) respectively, the mass loss for each stage being presented in Table I. Being organic compounds, the theoretical mass loss of excipients should be 100%, however in our case the mass loss in the case of organic excipients (32.37% CS, 43.1% C, 19.9 CC) is much smaller since the experiments were performed in nitrogen.

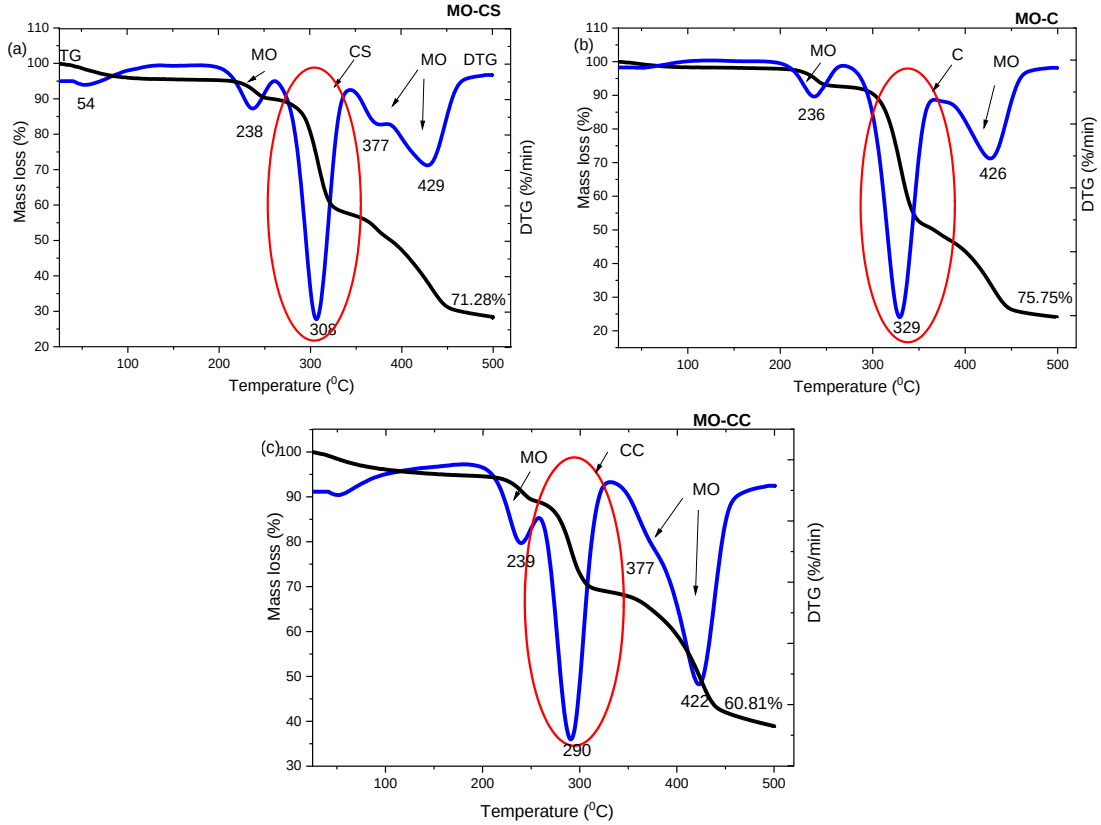

Figure 4.
TG and DTG curves of MO-CS (a), MO-C (b) and MO-CC (c)

Literature survey revealed that the decomposition of CS (same as C) take place in one stage, in the temperature range 300 - 400°C [8, 22], which confirm our results. L and S, in combination with MO, showed significant thermal changes as displayed in Figure 5a and Figure 5b.

In the case of MO-L, the peak at 135ºC is related to lactose dehydration, with a mass loss of 2.83%.

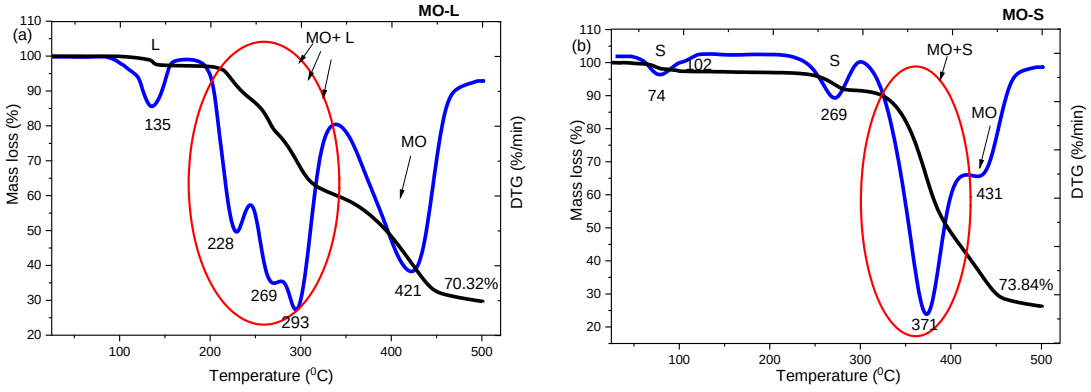

Figure 5.
TG and DTG curves of MO-L (a) and MO-S (b)

Powder X-ray diffraction

As presented in Figure 6, the XRD patterns of MO and binary physical mixtures of MO with different excipients are the sum of the patterns corresponding to each individual component, considering the mass ratio of 1:1 between MO and excipient, i.e. no physical or chemical interactions between the drug and excipients were observed.

The main features, as sharp diffraction peaks corresponding to MO (Figure 6a) were observed in all the MO-excipient mixtures, indicating that the crystalline structure of MO remained unchanged in the (1:1) physical mixtures. Additionally, the lack of shifting in the characteristic diffraction peaks of both ingredients in conjunction with a lack of new peaks indicated that neither physical interaction nor chemical reaction occurred between ingredients.

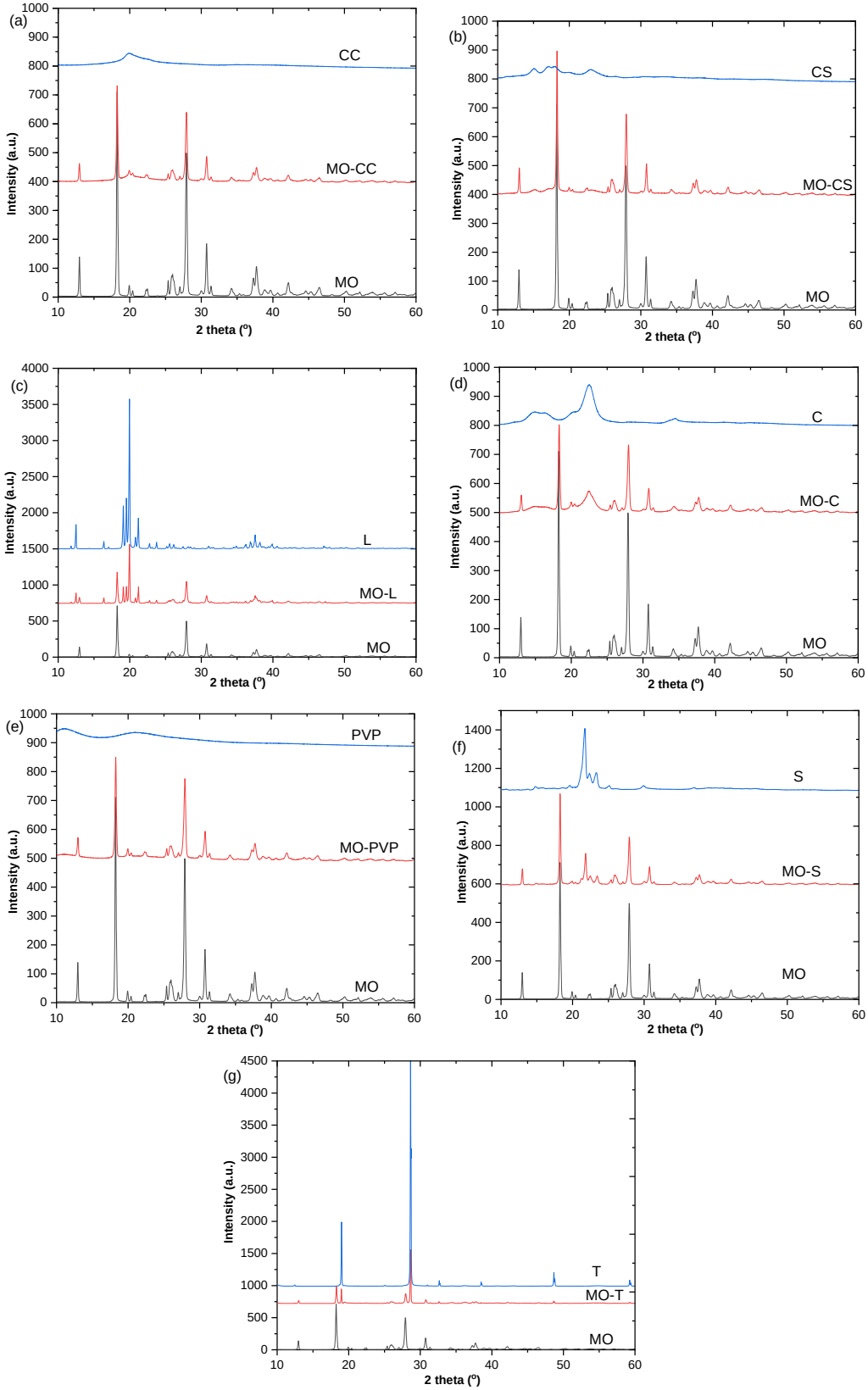

Figure 6.
XRD patterns of MO and binary mixture with: (a) CC; (b) CS; (c) L; (d) C; (e) PVP; (f) S and (g) T

The degree of crystallinity decreased in the following order: MO-L (92.7%) > MO-T (88.0%) > MO-PVP (83.4%) > MO-S (80.8%) > MO-CC (72.2%) > MO-CS (71.2%) > MO-C (68.4%), due to the lower degree of crystallinity of excipients comparing to MO, i.e. dissolution of MO in excipient: MO (92.9%) > T

(95.2%) > L (91.6%) > PVP (65.9%) > S (63.8%) > C (60.1%) > CS (57.2%) > CC (39.2%). XRD revealed that the crystalline nature of MO in formulations is stable.

FT-IR spectroscopy

The characteristic fingerprints of MO appear at 3474 cm^{-1} attributed to N–H bond vibration, at 3220 cm^{-1} attributed to C=C–H stretching vibration, at 2821 cm^{-1} attributed to C–H stretching, at 1672 cm^{-1} attributed to C=C stretching and at 1704 cm^{-1}attributed to C=O stretching [9]. Except the MO-T mixture, the FTIR spectra (Figure 7) of the binary mixtures contain the individual fingerprints of the MO and excipient, without any additional new absorption bands.

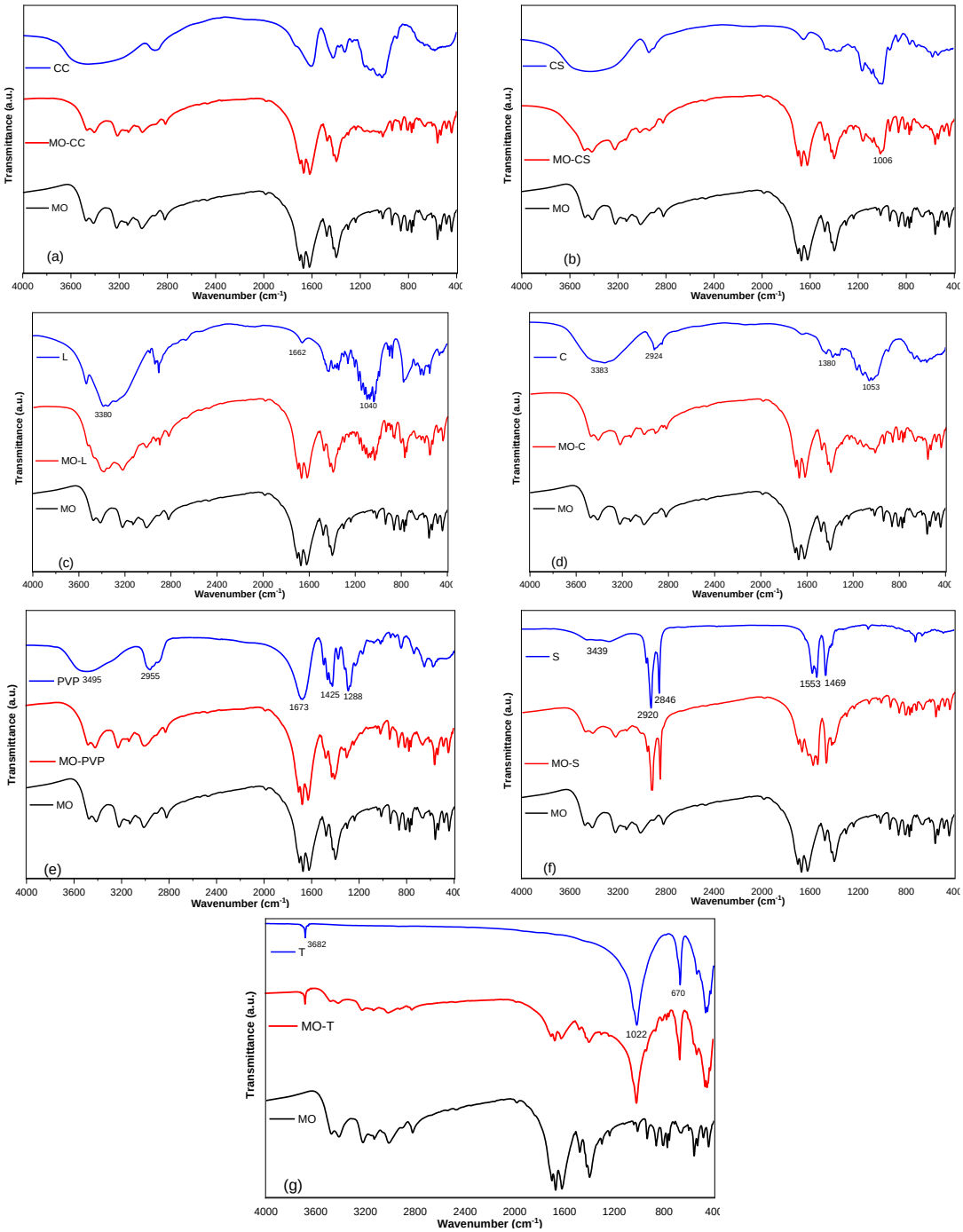

Figure 7.
FTIR spectra of MO, CC, CS, L, C, PVP, S, T and their binary mixtures

Table II

FTIR characteristic wavenumbers of magnesium orotate and excipients (croscarmellose (CC), corn starch (CS), lactate (L), magnesium stearate (S), microcrystalline cellulose (C), polyvinylpyrrolidone (PVP) and talcum (T)

Formulation	Wavenumber (cm^{-1})	Assignment of the vibration
MO	3474	N–H
	3220	C=C–H
	2821	C–H
	1704	C=O
	1672	C=C
CC	3430	O–H
	2923	C–H
	1061	C–O (ester groups)
	896	C–O–C
CS	3448	O–H
	2930	C–H
	1648	C–O
	1415	CH_2
	1158	C–O–C
	1019	C–O
	931, 864, 770	C–O–C ring
L	3378	O–H
	1658	C=O
	1469	COO^-
	1040	C–O
C	3383	O–H
	2920	C–H
	1384	O–H
	1058	C–O in glycosylic units of cellulose
PVP	3495	O–H (hydroxyl group)
	2955	O–H (carboxyl group)
	1673	C=O
	1425	O–H (hydroxyl group)
	1288	C–N
T	3682	O–H
	1022	Si–O–Si
	670	Si–O–Si

The FT-IR spectrum of CC (Figure 7a) is similar to that reported by Sarfraz *et al*. [29]. S (Figure 7b) presents a wide band at 3417 cm^{-1} attributed to the stretching vibration of the O–H bond and a band at 2918 cm^{-1} attributed to the C–H bond. At 1188 cm^{-1} and 1007 cm^{-1}, weak peaks appear associated with the rotation of the C–O bond [38]. The peak at 1006 cm^{-1} in the MO-CS mixture indicates minor interaction between MO and CS. L (Figure 7c) showed a wide band at 3380 cm^{-1} attributed to the stretching vibration of the O–H bond, a small peak at 1662 cm^{-1} attributed to the stretching vibration of the C=O bond and several peaks near 1040 cm^{-1} attributed to the rotational vibration of the C–O bond. This last peak also appears in the case of the MO-L mixture, which indicates minor interaction of the two components [30, 33]. Figure 7d showed a broad absorption region at 3383 cm^{-1} in the FT-IR spectrum of C attributed to the stretching vibration of the O–H bond and at 2920 cm^{-1} the peak is attributed to the valence vibration of the C–H bond in $–CH_2$. The weak peaks that appear near 1380 cm^{-1} are attributed to the shear vibrations of the O–H bond. The average peaks appearing near 1053 cm^{-1} are attributed to the C-characteristic bonds [11], i.e. to the deformation vibrations of the C–H bond, C–O for the glycosylic units of cellulose [6] and this excipient exerting a minor influence on the MO. Figure 7e showed the absence of absorption peaks specific to PVP in the MO-PVP mixture at 3495 cm^{-1} and at 2955 cm^{-1} (O–H valence vibration from the hydroxyl, respectively carboxyl group), at 1673 cm^{-1} (valence vibration of the C=O bond), at 1425 cm^{-1} (deformation vibration of the O–H bond from the hydroxyl group), at 1288 cm^{-1} (deformation vibration of the C–N bond) [5, 41]. The absence of the characteristic peaks of PVP in the MO-PVP mixture indicates good compatibility of this excipient with MO. In Figure 7f, S showed peaks at 3439 cm^{-1} (attributed to the valence vibrations of the O–H bond in the associated water molecules), at 2920 cm^{-1} and at 2846 cm^{-1} (attributed to the C–H valence vibrations). The twin peaks at 1553 cm^{-1} and at 1469 cm^{-1} are attributed to the symmetric and asymmetric COO^- vibrations [20]. The physical mixture of MO-S showed the absorption peaks of S, but also those of MO, indicating a week interaction between this excipient and MO. In Figure 7g, the FT-IR spectrum of T showed a small peak at 3682 cm^{-1} attributed to the O–H valence vibration, a strong peak at 1022 cm^{-1} attributed to the asymmetric valence vibration

of the Si–O–Si bond and an average peak at 670 cm^{-1} attributed to the symmetric valence vibration of the Si–O–Si bond [12]. The FT-IR spectrum of the binary mixture MO-T showed a summation of the peaks corresponding to each substance, while a significant decrease of the peak intensity belonging to MO can be noticed, suggesting the chemical interactions between MO and T, which implies a certain incompatibility.

The potential interactions between drugs and excipients are important features to be determined in order to obtain stable dosage forms with improved bioavailability. In the pre-formulation studies, it is important to use complementary thermo-analytical and spectroscopic methods, as the level of complexity observed in today's drug formulations requires a multidisciplinary approach. Thermal analysis is an important technique used to study the thermal behaviour of materials, with numerous advantages in the interaction studies between the active ingredient and excipients, study of degradation kinetics and stability of pharmaceutical forms, among other applications. The principle of the method is to monitor the changes in the sample weight as a function of temperature and time. Factors such as drug protection, reactions, intermediate and end-residue degradation products generated and degradation kinetics can be evaluated [43]. The thermal effects (DTA curves) appear like exothermic or endothermic peaks during the heating procedure, being related to different processes such as: crystallization, melting, vaporization, oxidation, decomposition reactions, solid state reaction or structural changes. The first derivative of the mass loss as a function of time (dm/dt) can be expressed as DTG curves.

In the thermal analysis of MO it was observed that the theoretical mass loss of MO with the formation of magnesium oxide is 88.02%. Since the thermal analysis was performed in nitrogen and the total mass loss (59.17%) is much lower than the theoretical value, we can say that the MO has not completely decomposed. In this case, due to the lack of oxygen, the decomposition of MO mainly generates intermediate organic compounds.

From the DTA curves, comparing the thermal effects of MO with mixtures, we can make an approximate classification of excipients into two categories: (1) excipients that do not affect the thermal behaviour of MO and decrease only slightly the decomposition temperatures of MO (such as T and PVP); and (2) excipients that strongly affect the decomposition and induce new thermal effects (CC, S, CS, C and L).

Analysing the DTA curve of MO-C it can be observed the appearance of a new endothermic peak at 332°C attributed to the decomposition of C, which is in concordance with previous results in literature [8]. On the other hand, the presence of endothermic peaks at 65°C for the MO-CS is attributed to the dehydration process due to the hydrophilic character of this polysaccharide. Decomposition of CS occurs at lower temperatures in comparison with MO, highlighted by the peaks at 310°C. The DTA curve of MO-CC mixture indicates an exothermic process at 292°C that occurs due to the combustion of CC with heat release. Three additional endothermic peaks were observed for the mixture MO-S, namely: two peaks at 77°C and 10°C due to loss of water molecules and one at 341°C characteristic for S decomposition. A similar thermal behaviour in the low temperature domain (25 – 11°C) was revealed for commercial S, as presented in literature [33]. MO-L presents several endothermic effects: the first one at 123°C attributed to dehydration of L, and a broader effect at 209°C with a shoulder at 224°C attributed to the L melting process and decomposition [1]. Moreover, L seems to interact with MO leading to the shift of 248°C endothermic peak toward 268°C.

According to the literature, as revealed by the TG and DTG curves, T begins to decompose at ~ 800°C, showing a wide endothermic signal at ~ 895°C, with the formation of instatite and amorphous silica is accompanied by a loss of mass of 5.23% [3]. Due to the good stability of T, the thermal behaviour of MO-T is attributed only to the decomposition of MO. The differences in weight loss (59.2% compared to 29.86%) come from the presence of uncompounded talc that remains in the heated mixture.

Under heat treatment, the mixture MO-PVP exhibits an increased mass loss in comparison to MO, suggesting that PVP brings its contribution to the mass loss. Excepting a small loss of water at 57°C, no significant changes in thermal effect was observed for PVP. However, due to large differences in the mass loss, we can conclude that the decomposition of PVP occurs in the same temperature ranges as MO. This behaviour is confirmed also by Onwudiwe *et al*. in a study devoted to ZnS nanoparticles stabilized in PVP, showing that the decomposition of PVP occurred between 378°C and 487°C with an endothermic peak at 430°C, very closed to MO [22].

According to the literature data [3, 14, 16], L melting point is 223ºC (α-lactate) and 252°C (β-lactate), and hence, we can affirm that the processes occurred in the temperature range 200 - 350°C (Figure 5) implies both the formation of a melting mixture between L and MO and decomposition reactions. As the temperature increase, TG and DTG curves reveals multiple inter-connected stages with mass loss of 9.6% and 27.62% at 228°C, 269°C and 293°C, suggesting the formation of intermediary organics derived from progressive decomposition of L. The results are in concordance with literature [40, 44]. MO melts at ~360°C followed by its decomposition with a mass loss of 30.27%. On the other hand, the decomposition of S and MO superimpose in the temperature range 300 - 500°C.

Summarizing the TG results, it can be state a good compatibility of MO-PVP and MO-T; a partial

compatibility for MO-CS, MO-C and MO-CC and incompatibility for MO-L and MO-S mixtures [10]. On the other hand, the non-destructive nature of XRD and FTIR spectroscopic methods makes them ideal tools for systematic drug–excipient compatibility assessment in the pre-formulation studies. It is well known that the percent of crystallinity can influence a drug's processing behaviour as well as its pharmacological performance [13, 28], being related to its solubility and dissolution [2, 36]. Additionally, the vibrational changes detected by FTIR method serve as direct evidence for potential intermolecular interactions among the dosage components. A reduction of the peak intensity, the appearance of new absorption peaks, indicates the existence of interactions between the excipient and the drug [30].

In our study, no significant decrease in intensity or change in the position of the diffraction peaks of the binary mixture in XRD was observed, indicating no solid states transition from crystalline to amorphous. Therefore, based on XRD pattern, no physical and chemical interactions between MO and excipients were noticed, as an indication of good compatibility. However, the FTIR spectroscopic features of MO in combination with the excipients revealed an incompatibility with T.

Comparing with the reported data in literature, a good compatibility was also reported for physical mixtures between simvastatin and different excipients (cellulose, lactate, ascorbic acid, magnesium stearate, citric acid and talcum powder) [15]. Similarly, good compatibility results were also reported for ketoprofen (KT) in combination with corn starch, microcrystalline cellulose, colloidal silicon dioxide, lactate and talc. In the case of KT-PVP and KT-S mixtures reported in literature, FT-IR and XRD analyses indicated possible interactions between the drug and the excipient, even at room temperature [35].

Conclusions

The evaluation of compatibility, in terms of physical and chemical interactions between MO and various excipients, in their physical mixtures (ratio 1:1 w/w) was investigated by the means of thermal analysis, XRD and FTIR spectroscopy. The modifications observed in the DTA curves, in terms of appearance of new peaks, expansion or displacement of the peaks to a lower temperature, indicated the interaction between MO and some of the investigated excipients. Based on the thermal analysis, it was noticed a good compatibility for the binary mixture MO-PVP and MO-T, partial compatibility for MO-CS, MO-C and MO-CC, and incompatibility between MO-L and MO-S. The XRD pattern of mechanical mixtures MO-PVP, MO-T, MO-CS, MO-C, MO-CC, MO-L and MO-S indicated that crystalline features of MO was preserved in all the mixtures, while no interactions (physical or chemical) between the drug and excipients occurred. Based on FT-IR spectroscopy, a week interaction between the components MO-CS, MO-S and MO-L was noticed, a strong one between and MO-T components, while a lack of interactions was observed between MO-PVP components, which was interpreted as a very good biocompatibility. So, by corroborating the results, we can conclude that PVP is the best choice as excipient for MO. The choice of excipients is an important step in the drug formulation process because it influences the release of the active substance from the pharmaceutical form. The lack of interactions between the active substance and the excipients favourably influences the bioavailability of the drug substance and the obtaining of safe drugs that can be used in therapeutical formulations.

Acknowledgement

This work was developed in the framework of the Romanian National Authority for Scientific Research CNCS-UEFISCDI, project number PN-III-P2-2.1-PED-2019-3664.

Conflict of interest

The authors declare no conflict of interest.

References

1. Bracconi P, Andrès C, N'diaye A, Pourcelot Y, Thermal analyses of commercial magnesium stearate pseudopolymorphs. *Thermochim Acta*, 2005; 429(1): 43-51.
2. Chella N, Narra N, Rama Rao T, Preparation and characterization of liquisolid compacts for improved dissolution of telmisartan. *J Drug Deliv.*, 2014; 2014; 692793: 1-10.
3. Chen J, Wang J, Li R, Lu A, Li Y, Thermal and X-ray Diffraction Analysis of Lactose Polymorph. *Procedia Eng.*, 2015; 102: 372-378.
4. De Baaij JHF, Hoenderop JGJ, Bindels RJM, Magnesium in man: Implications for health and disease. *Physiol Rev.*, 2015; 95(1): 1-46.
5. Dhumale VA, Gangwar RK, Datar SS, Sharma RB, Reversible aggregation control of polyvinylpyrrolidone capped gold nanoparticles as a function of pH. *Mater Express*, 2012; 2(4): 311-318.
6. Doncea SM, Ion RM, Fierascui RC, Bacalum E, Bunaciu AA, Aboul-Enein HY, Spectral methods for historical paper analysis: Composition and age approximation. *Instrum Sci Technol.*, 2009; 38(1): 96-106.
7. Gröber U, Schmidt J, Kisters K, Magnesium in Prevention and Therapy. *Nutrients*, 2015; 7(9): 8199-8226.
8. Hassani A, Hussain SA, Abdullah N, Kamaruddin S, Rosli R, Characterization of magnesium orotate-loaded chitosan polymer nanoparticles for a drug delivery system. *Chem Eng Technol.*, 2019; 42(9): 1816-1824.
9. Hîrjău M, Lupuliasa D, Rădulescu FS, Miron DS, The study of piroxicam dissolution from Eudragit RS-coated pellets. *Farmacia*, 2013; 61(5): 845-855.

10. Holandino C, Oliveira AP, Homsani F, Patrao de Paiva J, Moreno Barbosa G, de Lima Zanetti MR, de Barros Fernandes T, Monteiro Siqueira C, Feo da Veiga V, Louvisse de Abreu LC, Marzotto M, Bernardi P, Villano Bonamin L, Bellavite P, Linhares Rossi A, Henrique de Souza Piccian P, Structural and thermal analyses of zinc and lactose in homeopathic triturated systems. *Homeopathy*, 2017; 106(3): 160-170.
11. Kimani PK, Kareru PG, Madivoli S, Kairigo PK, Maina E, Rechab O, Comparative Study of Carboxymethyl Cellulose Synthesis from Selected Kenyan Biomass. *Chem Sci.*, 2016; 17(4): 1-8.
12. Li X, Zhang Y, He Y, Rapid detection of talcum powder in tea using FT-IR spectroscopy coupled with chemometrics. *Sci Rep.*, 2016; 6(1): 30313: 1-8.
13. Litteer B, Beckers D, Increasing Application of X-Ray Powder Diffraction in the Pharmaceutical Industry, Reprinted from American Laboratory News, June 2005.
14. Liu X, Liu X, Hu Y, Investigation of the Thermal Decomposition of Talc. *Clays Clay Miner.*, 2014; 62(2): 137-144.
15. Marian E, Jurca T, Kacso I, Borodi, G, Rus LM, Bratu I, Compatibility Study Between Simvastatin and Excipients in Their Physical Mixtures. *Rev Chim (Bucharest)*, 2015; 66(6): 803-807.
16. Marian E, Jurca T, Banică F, Morgova, C, Bratu I, Thermal Analysis and Raman Spectrometry of Some Complexes of Theophylline with Transitional Metals. *Rev Chim (Bucharest)*, 2010; 61(6): 596-574.
17. Moisa C, Vlad AM, Teusdea AC, Cadar O, Hoaghia MA, Stan RL, Taerel A, Jurca C, Vicaș LG, Randomized evaluation on the consumption of antibiotics in community pharmacies. *Farmacia*, 2018; 66(6): 1081-1090.
18. Moisa C, Hoaghia M, Simedru D, Cadar O, Influence of tablet formulation *in vitro* release of magnesium. *Stud UBabes-Bol Che.*, 2016; 3: 441-449.
19. Nikulin A, Potanina O, Alyussef M, Vasil'ev V, Abramovich R, Novikov O, Boyko N, Khromov A, Platonov E, Development of a technique for determining cadmium, lead, arsenic with the ETAAS method in medicinal plant raw materials. *Farmacia*, 2021; 69(3): 566-575.
20. Nep EI, Conway BR, Preformulation studies on grewia gum as a formulation excipient. *J Therm Anal Calorim.*, 2011; 108(1): 197-205.
21. Noah L, Pickering G, Mazur A, Dubray C, Hitier S, Dualé C, Impact of magnesium supplementation in combination with vitamin B6, on stress and magnesium status: secondary data from a randomized controlled trial. *Magnes Res.*, 2020; 33(3): 45-57.
22. Onwudiwe DC, Krüger TPJ, Jordaan A, Strydom CA, Laser-assisted synthesis and structural and thermal properties of ZnS nanoparticles stabilised in polyvinyl-pyrrolidone. *Appl Surf Sci.*, 2014; 321: 197-204.
23. Paus R, Prudic A, Ji Y, Influence of excipients on solubility and dissolution of pharmaceuticals. *Int J Pharm.*, 2015; 485(1-2): 277-287.
24. Pham PC, Pham PA, Pham SV, Pham PT, Pham PM, Pham PT, Hypomagnesemia: a clinical perspective. *Int J Nephrol Renovasc Dis.*, 2014; 7: 219-230.
25. Pickering RT, Bradlee ML, Singer MR, Moore LL, Higher Intakes of Potassium and Magnesium, but Not Lower Sodium, Reduce Cardiovascular Risk in the Framingham Offspring Study. *Nutrients*, 2021; 13(1): 269: 1-12.
26. Petibois C, Melin AM, Perromat A, Cazorla G, Déléris G, Glucose and lactate concentration determination on single microsamples by Fourier-transform infrared spectroscopy. *J Lab Clin Med.*, 2000; 135(2): 210-215.
27. Pop AL, Henteș P, Pali MA, Oșanu L, Ciobanu AM, Nasui BA, Mititelu M, Crișan S, Peneș ON, Study regarding a new extended-release calcium ascorbate and hesperidin solid oral formulation. *Farmacia*, 2022; 70(1): 151-157.
28. Rodríguez I, Gautam R, Tinoco AD, Using X-ray diffraction techniques for biomimetic drug development, formulation and polymorphic characterization. *Biomimetics (Basel)*, 2020; 6(1): 1: 1-23.
29. Sarfraz RM, Ahmad M, Mahmood A, Khan HU, Bashir S, Minhas MU, Sher M, Comparative study of various polymeric super disintegrants on the design and evaluation of novel antihypertensive orodispersible tablets. *Adv Polym Tech.*, 2016; 35(4): 378-385.
30. Segall AI, Preformulation: The use of FTIR in compatibility studies. *J Innov Appl Pharm Sci.*, 2019; 4(3): 01-06.
31. Seguel GV, Rivas BL, Paredes C, Synthesis and characterization of Zn(II) complex with the acetate and orotic acid MK ligands. *J Chil Chem Soc.*, 2010; 55(1): 5-7.
32. Siddiqui KA, Lama P, First orotic acid and isonicotinic acid based Zn complex: hydrothermal synthesis, crystal structure and thermogravimetric analysis. *J Struct Chem.*, 2018; 59(1): 166-171.
33. Shen DK, Gu S, The mechanism for thermal decomposition of cellulose and its main products. *Bioresource Technol.*, 2009; 100(24): 6496-6504.
34. Tita IC, Tita B, Toma CC, Marian E, Vicas LG, Thermal Behavior of Valsartan Active Substance and in Pharmaceutical Products. *Rev Chim (Bucharest)*, 2017; 68(10): 2307-2310.
35. Tița B, Fuliaș A, Bandur G, Marian E, Tița D, Compatibility study between ketoprofen and pharmaceutical excipients used in solid dosage forms. *J Pharm Biomed Anal.*, 2011; 56(2): 221-227.
36. Toderescu CD, Dinu-Pirvu C, Ghica MV, Anuta V, Popa DE, Vlaia L, Lupuliasa D, Influence of formulation variables on ketoprofen diffusion profiles from hydroalcoholic gels. *Farmacia*, 2016; 64(5): 728-735.
37. Verma H, Garg R, Development, optimization and characterization of chewable tablet containing synergistic combination of magnesium orotate dihydrate with cholecalciferol and menaquinone-7 for management of hyperglycemia and its pharmacokinetic study**.** *Magnes Res.*, 2021; 34(2): 43-63.
38. Wang Y, Xie W, Synthesis of cationic starch with a high degree of substitution in an ionic liquid. *Carbohyd Polym.*, 2010; 80(4): 1172-1177.
39. Weng J, Huang Y, Hao D, Ji Y, Recent advances of pharmaceutical crystallization theories. *Chin J Chem Eng.*, 2020; 28(4): 935-948.
40. Wesolowski M, Rojek B, Thermogravimetric detection of incompatibilities between atenolol and excipients using multivariate techniques. *J Therm Anal Calorim.*, 2013; 113(1): 169-177.

41. Zhang J, Yuan B, Ren H, Synthesis and Characterization of PVP/$Tb_{4/3}L{\bullet}7H_2O$ Luminescent Complex. *Earth Environ Sci.*, 2018; 170(3): 032043: 1-6.
42. Yeşilel OZ, Ölmez H, İçbudak H, Orotic acid complexes of Co(II), Ni(II), Zn(II) and Cd(II) with imidazole. *J Therm Anal Calorim.*, 2007; 89(2): 555-559.
43. Yoshida MI, Lima Gomes EL, Vianna Soares CD, Cunha AF, Oliveira MA, Thermal Analysis Applied to Verapamil Hydrochloride Characterization in Pharmaceutical Formulations. *Molecules*, 2010; 15(4): 2439-2452.
44. Qiao Y, Wang B, Ji Y, Xu F, Zong P, Zhang J, Tian Y, Thermal decomposition of castor oil, corn starch, soy protein, lignin, xylan, and cellulose during fast pyrolysis. *Bioresource Technol.*, 2019; 278: 287-295.